Dalton Transactions

Accepted Manuscript

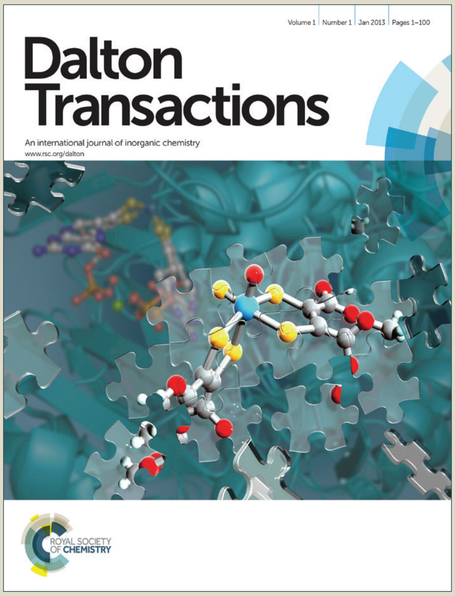

ROYAL SOCIETY OF CHEMISTRY

www.rsc.org/dalton

Exploration of new second-order nonlinear optical materials in the Cs-Hg-Br-I system

Qi Wu [a], *Yin Huang* [a], *Xianggao Meng* [b], *Cheng Zhong* [a] *, *Xingguo Chen* [a] *and Jingui Qin* *

Abstract A first example in the Cs-Hg-Br-I system, namely $Cs_2Hg_2Br_2I_4 \cdot H_2O$ (**1**)，has been synthesized by a reaction in solution. It belongs to a polar monolclinic space group *pc* with a= 7.460(5) Å, b= 13.458(9) Å, c= 8.891(6) Å, and β= 92.448(9)°. The basic anionic group in the crystal is non-centrosymmetric $[Hg_2Br_2I_4]^{2-}$, and the groups are aligned in the same direction in the crystal. As a result, **1** exhibits a phase-matchable SHG responses as strong as 6 time that of KDP. For the purpose of comparison, the known compound $Cs_2Hg_3I_8 \cdot H_2O$ (**2**) was also synthesized and its SHG property was studied for the first time. Band structure and optical property calculations for the two compounds based on DFT methods were also performed. The comprehensive properties of **1** and **2** as well as their analog, $Cs_2HgCl_2I_2$, have been compared and discussed.

Introduction

Nonlinear optical materials (NLO) are vital materials in optoelectronic technology owing to their applications in the photonic technologies. These materials always request good comprehensive properties. [1] For example, as NLO materials to be used in the infrared region (IR), large second harmonic generation (SHG) response, high laser damage threshold (LDT) and wide IR transparence region are all the important factors among the others.

Some efforts have been made to explore the halides and mixed halides as the NLO materials in the past decades by our group and other groups. Several halides such as $CsGeX_3$ (X=Cl, Br, I),[2] $CsCdBr_3$,[3] $RbCdI_3 \cdot H_2O$[4] $TIHgI_6$,[5] TI_3PbBr_5,[6] $HgBr_2$,[7] $Cs_2Hg_3I_8$,[8] Hg_2BrI_3,[9] $Cs_2HgCl_2I_2$,[10] Hg_2Br_3I,[11] and HgBrI[12] have been discovered to be potential candidates as new NLO optical crystals in IR region. Even though they have many advantages, the balance of SHG, LDT and IR transparent region still needs to be improved. The main problem is that large SHG and high LDT are normally conflicting properties. It is believed that a small bad gap is beneficial for a material to show strong NLO property [13], but at the meantime is harmful for material's optical stability and therefore lead to show low LDT, because the small band gap will cause easy and strong optical absorption leading to bad thermal and electronic effects including electron avalanche so as to cause laser damage. [14, 15] Therefore designing and synthesizing a compound which can balance the conflicting factors mentioned above is a very important and challenging task. For example, $Cs_2Hg_3I_8$ is an interesting compound which showed very strong SHG effect similar to KTP, but its band gap is small (2.56 eV), and its LDT was expected to be low. By introducing the Cl^- anion into $Cs_2Hg_3I_8$, our group has successfully obtained $Cs_2HgCl_2I_2$ whose band gap increased to 3.15eV ($Cs_2HgCl_2I_2$). Unfortunately, the SHG effect was greatly reduced to about a tenth of that of KTP or similar to KDP.

In this work, we are especially interested in exploring the Cs-Hg-Br-I system by replacing Cl^- of $Cs_2HgCl_2I_2$ with Br^-, or in other words, by partially replacing I^- of $Cs_2Hg_3I_8$ with Br^-. As a result, $Cs_2Hg_2Br_2I_4{\cdot}H_2O$ has been obtained. To the best of our knowledge, it is the first example in the Cs-Hg-Br-I system. For comparison, we have also synthesized the known compound $Cs_2Hg_3I_8{\cdot}H_2O$ which has never been reported with the NLO property. This paper reports the synthesis, crystal structure and optical properties, as well as the theoretical calculation analysis on the structure and optical properties. The results may have given us a useful clue on how to balance the comprehensive performance of halides as NLO materials by proper molecular design.

Experimental

Synthesis. $Cs_2Hg_2Br_2I_4{\cdot}H_2O$ (**1**): Stoichiometric amounts (2:1) CsBr (0.4256g, 2mmol) and HgI_2 (0.4544g, 1mmol) were carefully dissolved in a mixture of 5 ml distilled water and 40 ml acetone. The mixture was stirred at room temperature for 12 h, then the light yellow solution was volatilized at room temperature. A few days later, several block-shaped pale yellow transparent crystals of $Cs_2Hg_2Br_2I_4{\cdot}H_2O$ (0.6862g) were obtained (yield of 78 % based on the mass of HgI_2) and washed by cool acetone .

$Cs_2Hg_3I_8{\cdot}H_2O$ (**2**): The synthetic process is the same as the above except the starting materials are CsI (0.5196g, 2mmol) and HgI_2 (1.3632g, 3mmol), and the yield is 85% based on the mass of HgI_2.

Single-Crystal Structure Determinations. Single crystals of $Cs_2Hg_2Br_2I_4{\cdot}H_2O$ (1) and $Cs_2Hg_3I_8{\cdot}H_2O$ (2) with dimensions of $0.12 \times 0.10 \times 0.10$ mm^3 for (1) $0.20 \times 0.10 \times 0.10$ mm^3 for (2) were selected and used for the single-crystal X-ray diffraction experiment, respectively. Data sets were collected using a Bruker SMART APEX II diffractometer equipped with a CCD detector (graphite-monochromated Mo Kα radiation, λ = 0.71073 Å) at 296(2) K. Data set reduction and integration were performed using the software package SAINT PLUS.[16] The crystal structure are solved by direct methods and refined using the SHELXTL 97 software package.[17] During the refinement of compound (1), the refined results by SHELXTL gave a clue of twin component existed in the crystal. Then, the commands TWIN/BASF were used. For both compounds (1) and (2), the water hydrogen atoms were firstly located at their suitable positions according to the hydrogen-bonded environment around O atoms and then they were constrained to be at these sites. Given the very low flack parameters of 0.001(16) and 0.004(13) for the acentric compounds (1) and (2), their absolute structure could be determined. Single-crystal data collection, cell parameters, and basic information for $Cs_2Hg_2Br_2I_4{\cdot}H_2O$ and $Cs_2Hg_3I_8{\cdot}H_2O$ are summarized in Tables 1 and 2.

Physical Property Measurements X-ray powder diffraction (XRD) patterns of polycrystalline material were collected using a Bruker D8 Advanced dffractometer with Cu Kα1 radiation (λ = 1.54186 Å) in the range of 10°–70° (2θ) at a scanning rate of 0.5°/min. The experimental powder XRD dates of the two compounds are in good agreement with the caculated dates based on the single-crystal model. In addition, the powder XRD patterns for the two compounds are in good agreement with the reported dates (see in Figure S1 and S2 in the Supporting Information).

Thermogravimetric study was carried out on Setaram SETSYS-16 simultaneous analyzer instrument. The crystal sample was added into an Al_2O_3 crucible and heated at a rate of 10° C/min from room temperature to 600° C under a nitrogen atmosphere.

The IR spectrum was recorded on a NICOLET 5700 Fourier-transformed infrared

(FTIR) spectrophotometer in the 4000−700 cm^{-1} region (2.5−14 μm) using the attenuated total reflection (ATR) technique with a germanium crystal.

The Raman scattering spectrum in the 800 −100 cm^{-1} region (12.5 − 100 μm) was performed using a Renishaw RM 1000 laser confocal Raman microspectrometer at room temperature. The 514.5 nm line of an Ar-ion laser was used for excitation.

The UV-Vis absorption spectrum were performed on a Varian Cary 5000 UV-Vis-NIR spectrophotometer in the wavelength range of 200﹣800 nm. A $BaSO_4$ plate was used as the standard (100% reflectance). The absorption spectrum was calculated from the reflectance spectra using the Kubelka﹣Munk function: $\alpha/S = (1 - R)^2/2R$,[18] where α is the absorption coefficient, S is the scattering coefficient, and R is the reflectance.

Second-Order Nonlinear Optical Effect and Phase-Matching Behavior Measurements. The measurements of the powder frequency-doubling effects were carried out by means of the method of Kurtz and Perry.[19] A 1064 nm radiation generated by a Q-switched Nd: YAG solid-state laser was used as the fundamental frequency light. The sample was ground and sieved into several distinct particle size ranges (20 ~ 40，40 ~ 60，60 ~ 80，80 ~ 100，100 ~ 125，125 ~ 150, 150 ~ 200 and 200 ~ 250 μm). Samples of KDP were prepared as reference materials in identical fashion to estimate the SHG effect.

Computational Descriptions. In order to better comprehend the relationship between the optical property and the electronic structure for compounds 1 and 2. First-principles electronic structure calculations were performed. Single crystal structure data of the two compounds were used for calculations. Band structures and density of states (DOS) calculations were performed by using the first-principles quantum mechanical program CASTEP within the DFT formalism.[20] It is well known that the band-gap calculated by GGA is usually smaller than the experimental data due to the discontinuity of exchange-correlation energy. Thus, a scissors operator is used to shift upward all the conduction bands (CB) in order to agree with measured values of the band-gap. The interactions between the ionic cores and the electrons were described by the norm-conserving pseudopotentia.[21] The following orbital electrons were treated as valence electrons:

Cs-5s^{2}5p^{6}6s^1, Hg-5d^{10}6s^2, Br-4s^{2}4p^5, I-5s^{2}5p^5, O-2s^{2}2p^4 and H-1s^1. Revised versions of Perdew Burke┌Ernzerhof (RPBE) exchange-correlation function within the generalized gradient approximation (GGA) scheme was utilized in the total energy calculations.[22] The numbers of plane waves included in the basis sets were determined by a cutoff energy of 900 eV for the two compounds, and the numerical integration of the Brillouin zone was performed utilizing a 6 × 4 × 5 k -point Grid sampling for $Cs_2Hg_2Br_2I_4 \cdot H_2O$ and 6 × 6 × 6 for $Cs_2Hg_3I_8 \cdot H_2O$. Based on the optimized geometries of the $Cs_2Hg_2Br_2I_4 \cdot H_2O$ and $Cs_2Hg_3I_8 \cdot H_2O$ crystals, the linear optical refractive indices are calculated from the optical matrix transition elements between occupied and unoccupied states. The SHG coefficients are calculated by the improved calculation formula,[23] which has been successfully applied on a lot of NLO crystals such as BIBO,[24] $NaNO_2$,[25] and KDP.[26] The other parameters and convergent criteria were the default values of the **CASTEP** code .

Results and Discussion

Structural Description. The crystal structure of **1** is shown in Figure 1(a). There are two independent Hg^{2+} atoms. These two Hg^{2+} atoms form a $[Hg_2Br_2I_4]$ group (see Fig. 1b), where each Hg atom is bonded to two Br atoms and two I atoms forming a distorted tetrahedron, while both Br atoms are bridging atoms and four I atoms are dangling atoms. The bond lengths in the $[Hg_2Br_2I_4]$ group are listed in Table 2. Water molecule has been speculated to be hydrogen-bonded (all hydrogen-bonds are marked by gray dashed line in Fig. 1a), via hydrogen atoms H1A and H1B, to the bromine Br1 atom at (x, y, z-1) and iodine I3 atom at (x, y, z) and (x, 1-y, z-1/2), respectively. All the Hg-Br bond lengths (ranging from 2.757(3) to 3,203(4) Å) are longer than all the Hg-I bond lengths (ranging from 2.614(3) to 2,706(3) Å) because the formers are bridging bonds and the latters are dangling bonds. No any bond length in all four Hg-Br bond lengths and four Hg-I bond lengths is the same, leading the $[Hg_2Br_2I_4]$ group noncentrosymmetric. As shown in Fig. 1c, all the $[Hg_2Br_2I_4]$ groups are packed in a completely parallel direction (along c axis). It is this favorite packing style enables this crystal a net polarization and exhibiting strong SHG response.

Crystal structure of $Cs_2Hg_3I_8 \cdot H_2O$ was reexamined and is shown in Figure 2(a). There are two independent Hg^{2+} atoms and five independent iodine atoms, each Hg atom is bonded to four iodine atoms to form distorted $[HgI_4]$ tetrahedron (see Fig. 2b). Water molecule has been speculated to be hydrogen-bonded (all hydrogen-bonds are marked by gray dashed line in Fig. 2a), via hydrogen atoms H1A and H1B, to the iodine I4 atom at (x-1, y, z) and iodine I5 atom at (x, y, z), respectively. It is worthy mentioning that both the mirror and glide planes symmetries exist in the crystallographic structure of (2) with these atoms Hg2, I4, I5 and water O1 molecules residing in the mirror plane. It can be seen in Fig. 2a and 2c that I2 and I3 are the bridging atoms while I1, I4 and I5 are the ending atoms. All the dangling bonds (Hg-I1, Hg-I4 and Hg-I5) are shorter than the bridging bonds (Hg-I2 and Hg-I3). Fig. 2c shows the packing style of the $[HgI_4]$ tetrahedral. All the Hg-I1 and Hg-I4 are parallel to *c* axis. This packing style gives rise to a net polarization and leads to a substantial SHG response.

Nonlinear Optical Property. Powder SHG measurements using 1064 nm radiation revealed that $Cs_2Hg_2Br_2I_4{\cdot}H_2O$ and $Cs_2Hg_3I_8{\cdot}H_2O$ showed SHG efficiencies as strong as 6*KDP and 10*KDP, respectively. Study of the SHG intensity as a function of particle size (from 20 to 250 μm) for two materials is shown in Figure S3 and S4. The intensity of the SHG signals at first increases gradually with the increase of the sample size. And then it reaches a plateau at the maximum value after a certain particle size (of about 150 μm), which is a clear sign that the SHG of $Cs_2Hg_2Br_2I_4{\cdot}H_2O$ and $Cs_2Hg_3I_8{\cdot}H_2O$ are type 1 phase-matchable.[19]

Infrared Spectrum, Raman Spectrum, and UV− Vis Diffuse Reflectance Spectrum. The ATR-FTIR spectrum and Raman spectrum of polycrystalline **1** and **2** are shown in Figures S5-S8, respectively. They exhibit wide infrared transmission range from 2.5 to 50μm and 2.5 to 59μm, respectively, except obviously absorption peaks at 3700, 3500, and 1600 cm^{-1}, which are attributable to O-H vibrations in the water molecular. The UV−vis diffuse reflectance spectrum for the two compounds are shown in Figure S9 and S10. The spectrum shows that the absorption edge near the UV side for compound 1 is 440 nm, and compound 2 is 490nm. And this indicate that the band gap of the compound 1 and 2 are 2.82 and 2.59 eV, respectively, which means that the band gap can be improved by partially replacing I^- of the compound 2 with Br^-. And this is consistent with our design thought, which may be a useful method to explore other novel NCS materials which can balance large SHG properties and large band gap.

Thermogravimetric Analysis. Thermogravimetric (TGA) study was performed simultaneous on Setaram SETSYS-16 simultaneous thermal analyzer to investigate the thermal properties of the synthesized materials $Cs_2Hg_2Br_2I_4\cdot H_2O$ and $Cs_2Hg_3I_8\cdot H_2O$, As shown in Figures 3 and 4, TGA measurement results indicate that the compound 1 loss its water molecular at 160 ° C, from 160 ° C to 350 ° C, the compound continues to lose weight until about 39% remains. This implies that the residue is mainly CsI (whose weight portion in $Cs_2Hg_2Br_2I_4\cdot H_2O$ is 38%). The compound 2 is thermally stable up to 110 ° C when it starts losing water molecular. The two colorless crystals is not hygroscopic.

Theoretical Calculations. To gain further insights on the electronic structure and optical properties of $Cs_2Hg_2Br_2I_4\cdot H_2O$ and $Cs_2Hg_3I_8\cdot H_2O$, we performed theoretical calculations based on DFT methods using CASTEP.[20]

The partial density of states (PDOS) and total density of states (TDOS) for $Cs_2Hg_2Br_2I_4\cdot H_2O$ and $Cs_2Hg_3I_8\cdot H_2O$ are plotted in Figure S11 and S12. As is shown in Figure S11, it is found that the bands from -13.0 eV to -8.8 eV originate mainly from Br 4s, I 5s, O 2p and H 1s orbitals. The upper of the valence mainly contain Hg 6p, Br 4p and I 5p orbitals. The once empty Hg 6p orbital has lower energy, suggest bond formation between Hg and Br or I. The top of the valence band (VB) can be considered as long pair p electrons of I and Br. The bottom of Conduction Band (CB) is mainly composed of the orbitals of the Hg 6s，Br 4p (4s) and I 5p (5s) orbitals, which can be considered as anti-bond orbital between Hg and Br or I. This means that the $[HgBr_2I_2]^{2-}$ anionic group directly determines the band gap of the $Cs_2Hg_2Br_2I_4\cdot H_2O$.

From the Figure S12, it is found that the upper of the valence states mainly contain I 5p orbital. The 6p orbital of Hg is lower in energy suggest that the Hg-I sigma bond has lower energy than the long pair p electron of I as expected. The bottom of CB is mainly composed of the orbitals of the I 5p and Hg 5s which can be consider as the Hg-I anti sigma bond orbital. That is to say, the 5p of I to Hg-I anti-bond charge transfer transition of $[HgI_4]^{2-}$ anionic group directly correspond to the band gap of the $Cs_2Hg_3I_8\cdot H_2O$.

The electronic band structure of $Cs_2Hg_2Br_2I_4\cdot H_2O$ and $Cs_2Hg_3I_8\cdot H_2O$ are shown in Figure

S13 and S14. It is clear that $Cs_2Hg_2Br_2I_4 \cdot H_2O$ and $Cs_2Hg_3I_8 \cdot H_2O$ are indirect gap crystal with the band gap of 2.42 and 2.37eV, respectively, which are very close to the experimental value of 2.82 and 2.58eV. As is known to us, the band gap calculated by LDT is usually smaller than the experimental data owing to the discontinuity of exchange correlation energy, so the scissors operator of 0.403 and 0.208eV are adopted in our calculations in order to agree with the measured value of the band gap.

The calculated refractive indices and birefringence at several radiation wavelengths are shown in Figure S15 and S16. It exhibit that the birefringence Δn is 0.1 and 0.08 as the wavelength is longer than 1μm. This result is in agreement with the experimental result which indicated that the SHG effect is type 1 phase-matchable.

The point group of $Cs_2Hg_2Br_2I_4 \cdot H_2O$ and $Cs_2Hg_3I_8 \cdot H_2O$ belongs to m. And they have 10 nonvanishing tensors of second order susceptibility. Under the restriction of Kleinman's symmetry, only 6 independent SHG tensors are left. The SHG coefficients are half of the independent SHG tensors, so the theoretical SHG coefficients of the compounds $Cs_2Hg_2Br_2I_4 \cdot H_2O$ and $Cs_2Hg_3I_8 \cdot H_2O$ are as follows: d_{11}=8.65 pm/V, d_{15}=-4.56 pm/V, d_{26}=-5.30 pm/V, d_{35}=-2.17 pm/V, d_{24}=4.34 pm/V and d_{33}=1.95 pm/V for $Cs_2Hg_2Br_2I_4 \cdot H_2O$, d_{11}=-24.40 pm/V, d_{15}=-4.99 pm/V, d_{26}=12.3 pm/V, d_{35}=13.7 pm/V, d_{24}=18.98 pm/V and d_{33}=17.09 pm/V for $Cs_2Hg_3I_8 \cdot H_2O$. These results are very close to our experimental observation that $Cs_2Hg_3I_8 \cdot H_2O$ and $Cs_2Hg_2Br_2I_4 \cdot H_2O$ exhibit strong second-harmonic generation (SHG) of about 6*KDP (d_{36}=0.39 pm/V) and 10*KDP, respectively.

Conclusions

This paper explores the novel Cs-Hg-Br-I system by replacing Cl^- of $Cs_2HgCl_2I_2$ with Br^-, or in other words, by partially replacing I^- of $Cs_2Hg_3I_8$ with Br^- in the hope to improve the balance between the NLO property and the band gap and to search for new NLO materials with better comprehensive performance. As a result, the synthesis, crystal structure and optical properties of a new compound $Cs_2Hg_2Br_2I_4 \cdot H_2O$ has been studied. The comparison of the properties indicates that $Cs_2Hg_2Br_2I_4 \cdot H_2O$ has shown powder SHG effect 6 times that of $Cs_2HgCl_2I_2$ while its band gap is higher than that of $Cs_2Hg_3I_8 \cdot H_2O$. The results have given us an useful information and will be helpful for designing new NLO materials with better comprehensive performances.

Acknowledgments

This work was financially supported by the National Basic Research Project of China (No. 2010CB630701) and the Natural Science Foundation of China (No. 91022036).

Notes and references

a Department of Chemistry, Wuhan University, Wuhan 430072, China

b College of Chemistry, Central China Normal University, Wuhan 430079, China

† Electronic Supplementary Information (ESI) available: X-ray crystallographic files in CIF format, X-ray diffraction powder patterns, Phase-matching curves, ATR-FTIR spectrum, Raman spectrum, UV-Vis absorption spectrum, total and partial density of states, the band structure, calculated refractive Indices at selected wavelengths for two compounds. The CCDC reference numbers of compounds 1 and 2 are 933106 and 933107.

1. (a) C. Chen and G. Liu, *Annu. Rev. Mater. Sci.*, 1986, **16**, 203; (b) P. S. Halasyamani and K. R. Poeppelmeier, *Chem. Mater.*, 1998, **10**, 2753; (c) K. M. Ok and P. S. Halasyamani, *Chem. Soc. Rev.*, 2006, **35**, 710.
2. (a) J. Zhang, N. Su, C. Yang, J. Qin, N. Ye, B. Wu and C. Chen, Proc. SPIE., 1998, 1, 3556. (b) M. D. Ewbank, F. Cunningham, R. Borwick, M. J. Rosker, P. Gunter, Proceedings of CLEO’97 CFA, 1997, 7, 462. (c) L. C. Tang, J. Y. Huang, C. S. Chang, *J. Phys.: Condens. Matter.*, 2000, **12**, 9129.
3. P. Ren, J. Qin, C. Chen, *Inorg. Chem.*, 2003, **42,** 8.
4. P. Ren, J. Qin, T. Liu, Y, Wu.; C, Chen, *Optical Materials.*, 2003, **23**, 331.
5. K. I. Avdienko, D. V. Badikov, V. V. Badikov, V. I. Chizhikov, V. L. Panyutin, G. S. Shevyrdyaeva, S. I. Scherbakov, E. S. Scherbakova, *Opt. Mater.*, 2003, **23**, 569.
6. A. Ferrier, M. Velazquez, X. Portier, R. Moncorge, *J. Cryst. Growth.*, 2006, **289**, 357.
7. T. Liu, J. Qin, G. Zhang, T. Zhu, F. Niu, Y. Wu, C. Chen, *Appl. Phys. Lett.*, 2008, 93, 091102.

8. G. Zhang, J. Qin, T. Liu, T. Zhu, P. Fu, Y. Wu, C. Chen, *Cryst. Growth Des*., 2008, **8**, 2946.
9. Y. Li, M. Wang, T. Zhu, X. Meng, C. Zhong, X. Chen, J. Qin, *Dalton Trans*., 2012, **41**, 763.
10. G. Zhang, Y. Li, K. J, H. Z, T. Liu, X. Chen, J. Qin, Z. L, P. F, Y. Wu, C. Chen, *J. Am. Chem. Soc.*, 2012, **134**, 14818.
11. Y. Huang, X. Meng, L. Kang, Y. Li, C. Zhong, Z. Lin, X. Chen, J. Qin, *CrystEngComm*., 2013, **15**, 4196.
12. Q. Wu, Y. Li, H. Chen, K. Jiang, H. Li, C. Zhong, X. Chen, J. Qin, *Inorganic Chemistry Communications*., 2013, **34**, 1.
13. A. G. Jackson, M. C. Ohmer, S. R. LeClair, *Infrared Physics & Technology*., 1997, **38**, 233.
14. X. Lin, G. Zhang and N. Ye, *Crystal Growth & Design,* 2009, **9**, 1186
15. W. Yin, K. Feng, R. He, D. Mei, Z. Lin, J. Yao and Y. Wu, *Dalton Trans.,* 2012, **41**, 5653
16. G. M. Sheldrick, *SHELXTL, version 6.14*, Bruker Analytical X-ray Instruments, Inc., Madison, WI, USA, 2003.
17. G. M. Sheldrick, *Acta Crystallogr*., 2008 , **A64**, 112.
18. W. M. Wendlandt, H. G. Hecht, Reflectance Spectroscopy; Interscience: New York, 1966; pp 62 − 65.
19. S. K. Kurtz, T. T. Perry, *J. Appl. Phys*., 1968 , **39**, 3798.
20. S. J. Clark, M. D. Segall, C. J. Pickard, P. J. Hasnip, M. J. Probert, K. Refson, M. C. Payne. *Z. Kristallogr*., 2005, **220**, 567.
21. M. C. Payne, M. P. Teter, D. C. Allan, T. A. Arias, J. D. Joannopoulos. *Rev. Mod. Phys*., 1992, **64**, 1045.
22. J. P. Perdew, K. Burke, M. Ernzerhof, *Phys. Rev. Lett*., 1996, **77**, 3865.
23. C. Chen, Z. Lin, Z. Wang, *Appl. Phys. B: Lasers Opt*., 2005, **80**, 1.
24. Z. Lin, Z. Wang, C. Chen, M.H. Lee, *J. Appl. Phys*., 2001, **90**, 5585.
25. Z. Lin, Z. Wang, C. Chen, M.H. Lee, *Acta Phys. Sin*., 2001, **50**, 1145.
26. Z. Lin, Z. Wang, C. Chen, M.H. Lee, *J. Chem. Phys*., 2003, **118**, 2349.

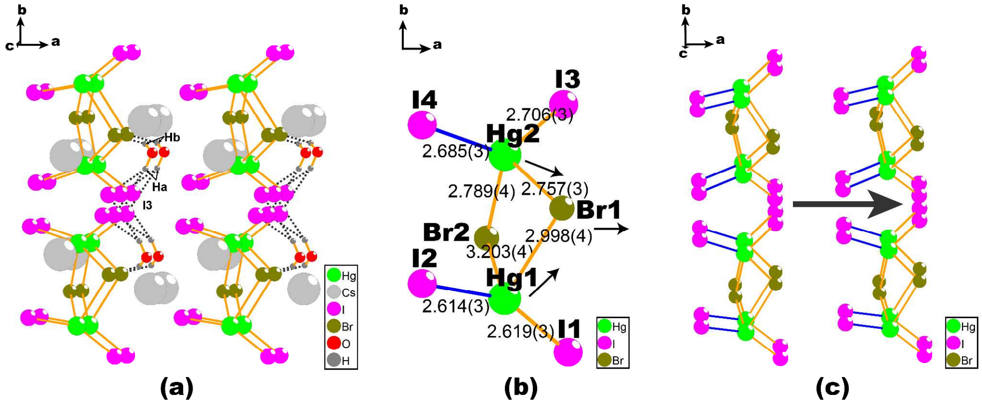

Figure 1. (a) Ball-and-stick diagrams of $Cs_2Hg_2Br_2I_4\cdot H_2O$. (b) Ball-and-stick diagrams of $[Hg_2Br_2I_4]$ group. (c) The favorite packing of $[Hg_2Br_2I_4]$ groups in the crystal.

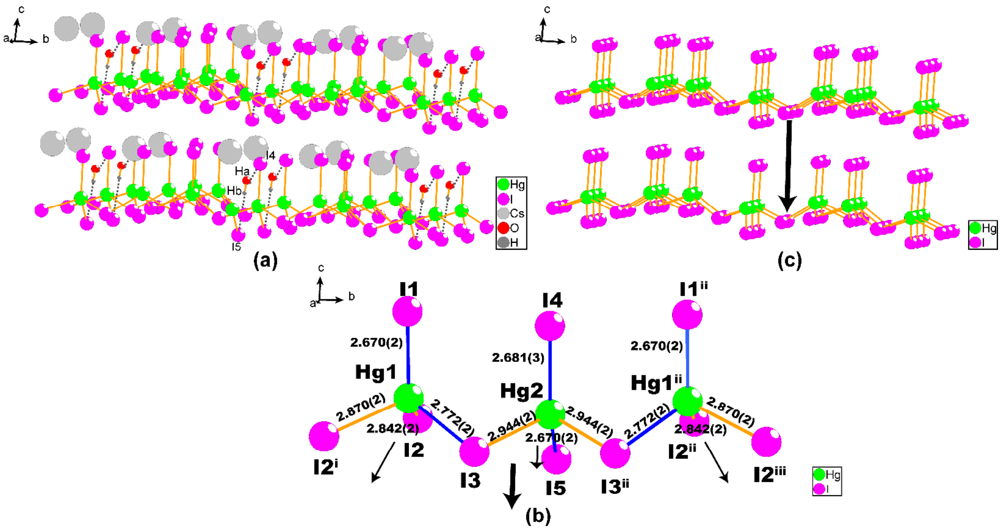

Figure 2. (a) Ball-and-stick diagrams of $Cs_2Hg_3I_8 \cdot H_2O$. (b) HgI_4 tetrahedral groups (Each Hg^{2+} is bonded to four iodine atoms with two shortest (blue) and two longer (yellow) bond distances, Å). Symmetry codes: i) ½ +x, ½ -y, z; ii) x, 1-y, z; iii) ½ +x, ½ +y, z. (c) Ball-and-stick diagrams of $Cs_2Hg_3I_8 \cdot H_2O$ (Cs, O, H atom are omitted for clarity).

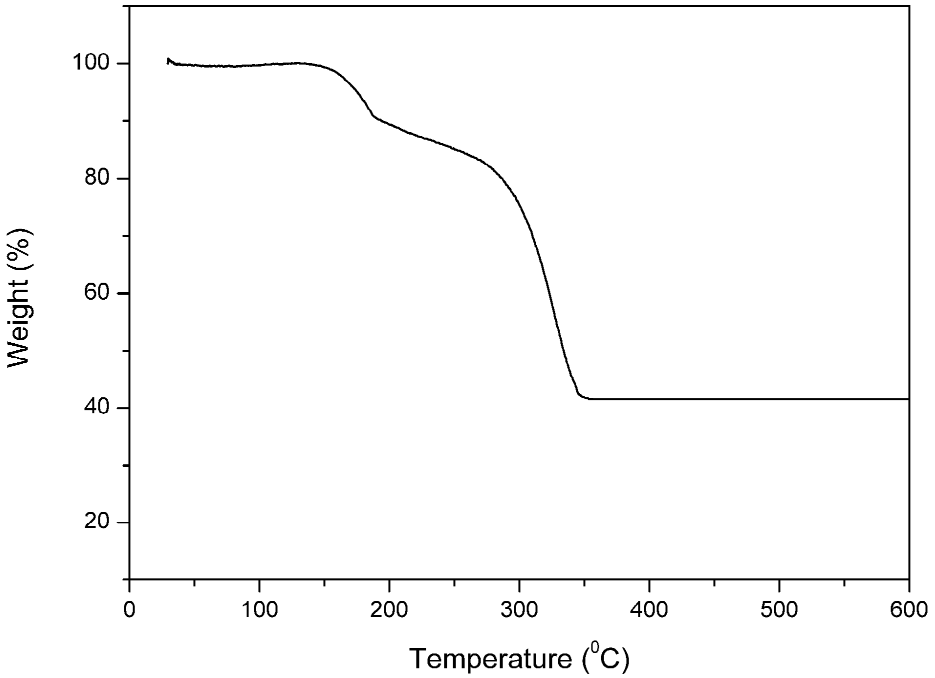

Figure 3. Thermogravimetric analysis curve for $Cs_2Hg_2Br_2I_4{\cdot}H_2O$ crystal.

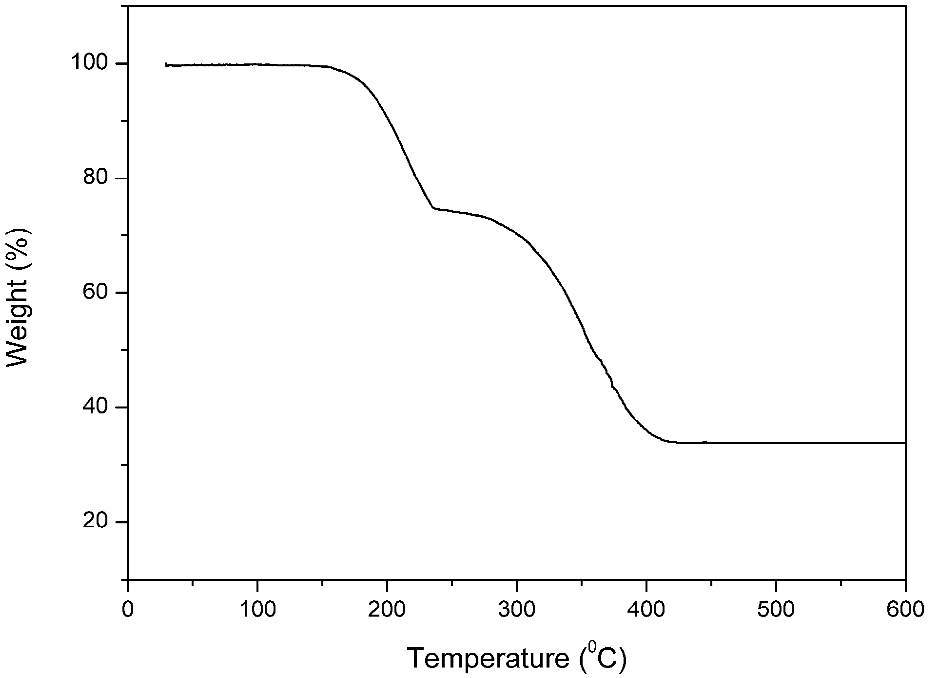

Figure 4. Thermogravimetric analysis curve for $Cs_2Hg_3I_8{\cdot}H_2O$ crystal.

Table 1. crystallographic Data for $Cs_2Hg_2Br_2I_4\cdot H_2O$ and $Cs_2Hg_3I_8\cdot H_2O$

Formula	$Cs_2Hg_2Br_2I_4\cdot H_2O$	$Cs_2Hg_3I_8\cdot H_2O$
Fw	1352.44	1900.81
T/K	296(2) K	296(2) K
Wavelength/Å	0.71073	0.71073
Crystal system	Monoclinic	Monoclinic
Crystal color	Light yellow	Deep yellow
Space group	Pc	cm
a/Å	7.460(5)	7.430(3)
b/ Å	13.458(9)	21.644(7)
c/ Å	8.891(6)	7.671(3)
α(◦)	90	90
β(◦)	92.448(9)	107.962(4)
γ (◦)	90	90
Volume/$Å^3$	891.9(10)	1173.6(7)
Z	2	2
D_{cacl}/g cm^{-3}	5.036	5.379
F(000)	1124	1568
Reflections collected	5065	3841
Independent reflections	2364	1906
R_1, wR_2 $[I > 2\sigma(I)]$	0.0501/0.0978	0.0466/0.1054
R_1, wR_2 (all data)	0.0715/ 0.1082	0.0613/0.1140
Flack parameter	0.001(16)	0.004(13)
Min/max $\Delta\rho$/$eA^{\circ -3}$	-1.703/1.051	-1.970/1.945

Table 2. Selected bond distances for $Cs_2Hg_2Br_2I_4 \cdot H_2O$ (1) and $Cs_2Hg_3I_8 \cdot H_2O$ (2).

Compound	Bond	Distance (Å)	Bond	Distance (Å)
1	Hg(1)-I(1)	2.619(3)	Hg(2)-I(3)	2.706(3)
	Hg(1)-I(2)	2.614(3)	Hg(2)-I(4)	2.685(3)
	Hg(1)-Br(1)	2.998(4)	Hg(2)-Br(1)	2.757(3)
	Hg(1)-Br(2)	3.203(4)	Hg(2)-Br(2)	2.789(4)
2	Hg(1)-I(1)	2.670(2)	Hg(2)-I(5)	2.670(3)
	Hg(1)-I(3)	2.772(2)	Hg(2)-I(4)	2.681(3)
	Hg(1)-I(2)	2.842(2)	Hg(2)-I(3)	2.944(2)
	Hg(1)-I(2)^{i}	2.870(2)	Hg(2)-I(3)^{ii}	2.944 (2)

Symmetry codes: i) ½ +x, ½ -y, z; ii) x, 1-y, z for compound (2).

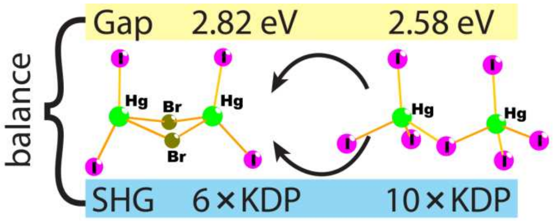

A new compound $Cs_2Hg_2Br_2I_4{\cdot}H_2O$ was synthesized to achieve a better balance between nonlinear optical property and band gap.